A rapid bioanalytical tool for detection of sequence-specific circular DNA and mitochondrial DNA point mutations

Article *in* Analytical and Bioanalytical Chemistry · February 2019

DOI: 10.1007/s00216-019-01683-8

CITATIONS
5

READS
137

4 authors, including:

Yuqian Zhang
Mayo Clinic
15 PUBLICATIONS **287** CITATIONS
SEE PROFILE

Ahmet Kaynak
University of Cincinnati
14 PUBLICATIONS **66** CITATIONS
SEE PROFILE

Leyla Esfandiari
University of Cincinnati
33 PUBLICATIONS **243** CITATIONS
SEE PROFILE

Analytical and Bioanalytical Chemistry
https://doi.org/10.1007/s00216-019-01683-8

COMMUNICATION

A rapid bioanalytical tool for detection of sequence-specific circular DNA and mitochondrial DNA point mutations

Yuqian Zhang [1] · Ahmet Kaynak [2] · Taosheng Huang [3] · Leyla Esfandiari [1,2]

Received: 17 December 2018 / Revised: 4 February 2019 / Accepted: 8 February 2019

Abstract

Mutations in mitochondrial DNA (mtDNA) have been an essential cause of numerous diseases, making their identification critically important. The majority of mtDNA screening techniques require polymerase chain reaction (PCR) amplification, enzymatic digestion, and denaturation procedures, which are laborious and costly. Herein, we developed a sensitive PCR-free electrokinetic-based sensor combined with a customized bis-peptide nucleic acid (bis-PNA) and gamma-PNA (γ-PNA) probes immobilized on beads, for the detection of mtDNA point mutations and sequence-specific supercoiled plasmid DNA at the picomolar range. The probes are capable of invading the double-stranded circular DNA and forming a stable triplex structure. Thus, this method can significantly reduce the sample preparation and omit the PCR amplification steps prior to sensing. Further, this bioanalytical tool can open up a new paradigm in clinical settings for the screening of double-stranded circular nucleic acids with a single-base mismatch specificity in a rapid and sensitive manner.

Keywords Bis-PNA · Gamma-PNA · Mitochondrial DNA · Circular double-stranded DNA · Electrokinetic sensor

Introduction

The mitochondrion, a double-membrane organelle, is responsible for producing the adenosine triphosphate (ATP) and metabolites to fulfill the cellular energy. The human mitochondrion has its own genetic system containing a double-stranded circular DNA [1]. A variety of human diseases related to the mitochondrial DNA (mtDNA) mutations has been discovered including Alzheimer's disease, Parkinson's disease, and breast cancer to name a few [2]. Thus, examination of mtDNA point mutations and deletions has been emerging as a diagnostic genetic marker. Moreover, the human mtDNA genome has a high copy number per cell, is maternal inheritance, and has high sequence variability [3], which makes its analyses particularly useful as a genetic fingerprinting for human identification in the criminal justice [4] and identification of the missing in action (MIA) in the military [5].

Different techniques have been exploited to detect mtDNA mutations such as the denaturing high-performance liquid chromatography (DHPLC) [6], the temperature gradient gel electrophoresis (TTGE) [7], and the pyrosequencing and SNaPshot technologies [8]. Currently, the next-generation sequencing (NGS) [9] and the DNA microarrays [10] are the state-of-the-art techniques for the detection of mtDNA single-nucleotide polymorphisms (SNPs). While these technologies are highly accurate, they require time-consuming and expensive amplification steps along with labeling and enzymatic reactions. Also, these techniques require relatively expensive equipment and are mainly set up in hospitals and national laboratories. Thus, advancement in nano/microscale technologies could significantly contribute to mtDNA screening by minimizing the sample preparation and amplification which could reduce time, labor, and cost while providing field deployability. Despite the advantages, there have been only few reports on utilizing nanotechnologies for the detection of SNPs in mtDNA [11–16]. For instance, Taylor et al. demonstrated a single-stranded conformation polymorphism (SSCP)

✉ Leyla Esfandiari
esfandla@ucmail.uc.edu

[1] Department of Electrical Engineering and Computer Science, University of Cincinnati, Cincinnati, OH 45221, USA

[2] Department of Biomedical Engineering, University of Cincinnati, Cincinnati, OH 45221, USA

[3] Department of Human Genetics, Cincinnati Children's Hospital, Cincinnati, OH 45229, USA

Published online: 27 February 2019

analysis to quantitatively assess the mtDNA heteroplasmy via a DNA self-assembly microfluidic chip [11]. Another SNP detection platform developed by Yang's group in which surface-enhanced Raman spectroscopy (SERS) was utilized to detect the single-stranded mtDNA binding events [12]. Although these technologies are highly sensitive and selective, they still require laborious enzymatic digestion, DNA denaturation, and tedious device fabrication prior to detection. Thus, there is a demand for a mtDNA detection scheme with simple and low-cost fabrication and sample preparation criteria to precisely detect the mutation in a timely manner while maintaining the specificity, sensitivity, and reproducibility of the results.

We have previously developed a low-voltage, miniaturized electrokinetic-based sensor combined with a highly sensitive peptide nucleic acid (PNA) hybridization assay for the detection of sequence-specific nucleic acids including single-stranded DNA (ssDNA), ribosomal RNA (rRNA), and microRNA (miR) at the femtomolar (fM) concentration detection limit [17–20]. This technology omits the need for PCR amplification as the detection signal gets intrinsically amplified by a highly sensitive bead-based assay blocking the ionic current across a solid-state nanopore-based sensor. Also, as the bead harboring the target nucleic acids blocks the pore, the signal duration is extended to tens of milliseconds which can be easily detected with a simple and low-cost operational amplifier. Therefore, this simple yet powerful sensor has the potential to be easily integrated with microfluidics for a complete point-of-care (POC) diagnostic.

Here, to take this PCR-free detection scheme a step further and develop a semi-automated mtDNA sensor, we have omitted the time-consuming sample pretreatment procedure including the DNA digestion and denaturation by designing a new set of bis-PNA and γ-PNA assays to detect a segment of the circular double-stranded DNA with high specificity. As a model system for circular DNA, the pTS12 plasmid was constructed with the insertion of a known oligonucleotide DNA sequence into the pUC19 plasmid and the concentration detection limit of 10 pM was established. Furthermore, to investigate the single-base mismatch specificity of our system, skin-derived double-stranded mtDNA with a known point mutation was detected. Successful detection of the supercoiled DNA with mutations illustrated that this bioanalytical tool can be used as a semi-automated sensor by minimizing the sample pretreatment and, thus, can significantly reduce the time and cost while maintaining the sensitivity. Therefore, in the future, this miniaturized, low-power, and PCR-independent sensor can be integrated with microfluidics to be evolved as a rapid, cost-effective, and portable mtDNA diagnostic in the clinical settings and SNP typing in the forensic science.

Material and methods

Materials

All chemicals were purchased from Sigma-Aldrich (St. Louis, MO) unless otherwise noted. Carboxylic acid-functionalized polystyrene beads with 3-μm diameter were purchased from Bangs Laboratories, Inc. (Fisher, IN). Borosilicate filaments with an outer diameter of 1 mm and an inner diameter of 0.78 mm were obtained from Sutter Instrument (Novato, CA). NovaBlue competent *Escherichia coli* K-12 cells, carbenicillin, and Clonables Ligation/Transformation Kit were purchased from EMD Millipore, Inc. (Billerica, MA). UView™ 6× Loading Dye, 50× Tris/Acetic Acid/EDTA (TAE), and Certified™ Molecular Biology Agarose were obtained from Bio-Rad (Hercules, CA). The pUC19 plasmid was purchased from Oxford Genetics (Oxford, UK). Restriction endonucleases (S*ma*I, N*co*I, X*mn*I, E*co*RI, S*ap*I and S*sp*I), SYBR® Safe DNA Gel Stain, Rapid DNA Ligation Kit, and S.O.C. Medium were purchased from Thermo Fisher, Inc. (Waltham, MA). QIAprep Spin Miniprep Kit and Gentra Puregene Tissue Kit were purchased from QIAGEN (Germantown, MD). The probes were designed using the Primer 3 program and specificity was checked using the NCBI Blast program. Two 5′-phosphorylated oligonucleotides (5′-CCA TGG AGA AGA AAG GAG AAA-3′ and 5′-TTT CTC CTT TCT TCT CCA TGG-3′) and the bis-PNA probe for plasmid detection (NH_2-OOO-JJT TTJ TTJ T-OOO-TCT TCT TTC C–KK) were purchased from Bio-Synthesis, Inc. (Lewisville, TX). γ-PNA probe for the detection of mtDNA (NH_2-OOOO-TTAC*-CGG*-GCT*-CCA*-TCT) was synthesized and purified by PNA Bio (Newbury Park, CA). MtDNA samples were kindly provided by Dr. Huang's group from Cincinnati Children's Hospital, Department of Human Genetics.

Preparation of samples

Plasmid construction

Plasmid pTS12 was constructed based on the commercial pUC19 plasmid standard molecular biology protocol [21]. In brief, pUC19 was digested with restriction enzyme (S*ma*I) and formed the open circular morphology, the digested plasmid was suspended into 1.5 mL of annealing buffer (10 mM Tris(hydroxymethyl) aminomethane, 50 mM NaCl, 1 mM EDTA, pH 7.5) in a microfuge tube containing the two complementary phosphorylated oligonucleotides and placed into 95 °C water bath for 15 min. After cooling to the room temperature, the annealed oligonucleotides were inserted into pUC19 which resulted in the construction of the pTS12 plasmid (Fig. 1a).

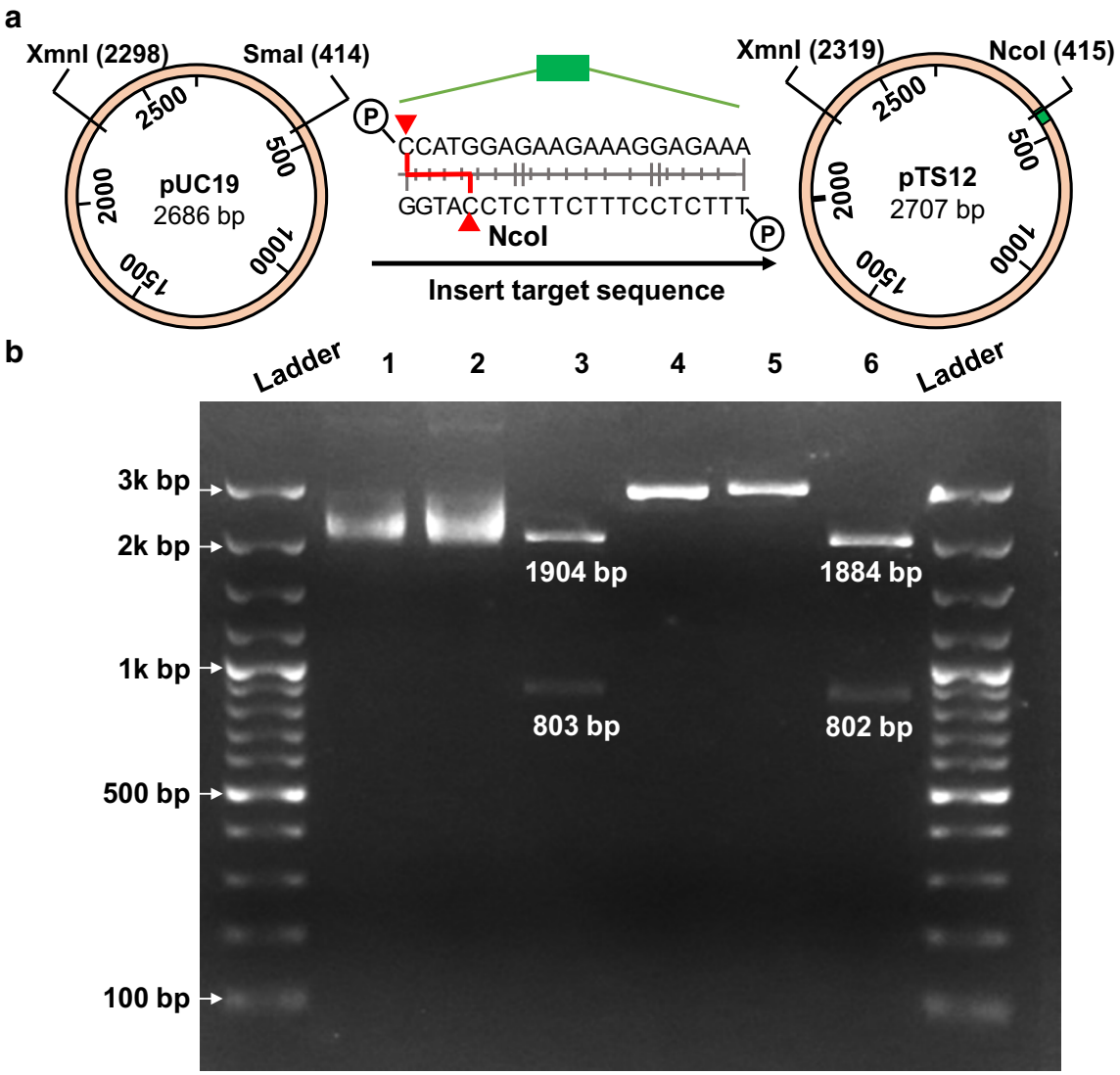

Fig. 1 **a** Recombinant pTS12 plasmid was constructed by enzymatically digesting the pUC19 plasmid (2686 base pairs) followed by the insertion of the target sequence resulted in the formation of the pTS12 plasmid with 2707 base pairs. **b** Agarose gel electrophoresis of pTS12 and pUC19 and their digested fragments. Lane 1: intact pUC19 plasmid; lane 2: intact pTS12 plasmid; lane 3: pTS12 cut with *Nco*I and *Xmn*I restriction enzymes; lane 4: pUC19 cut with *Nco*I and *Xmn*I restriction enzymes; lane 5: pTS12 cut with *Sma*I and *Xmn*I restriction enzymes; lane 6: pUC19 cut with *Sma*I and *Xmn*I restriction enzymes

Competent *E. coli* K-12 cells (NovaBlue) were transformed with pTS12 vector following the Novagen protocol. After the transformation, a white single colony containing recombinant plasmid was selected via the blue-white screening technique and cultured. The cultured plasmids were extracted and purified with the QIAprep Spin Miniprep Kit. The concentration and purity of the extracted plasmids were measured using a NanoVue Plus spectrophotometer (GE Healthcare, Chicago, IL).

Assessment of oligonucleotide insertion

To verify the successful construction of pTS12, plasmids were digested at selected sites and the DNA fragments were evaluated by gel electrophoresis. Intact plasmids and digested plasmids were separately loaded into 1.25% agarose gel in TAE buffer (40 mM Tris base, 20 mM sodium acetate, 2 mM EDTA, pH 8.3) and 80 V was applied for 1 h using the Mini-Sub® Cell GT Horizontal Electrophoresis System (Bio-Rad, Hercules, CA). Figure 1b shows the intact pUC19 (lane 1) and pTS12 (lane 2) as supercoiled constructs. pTS12 and pUC19 were double digested with *Sma*I, *Nco*I, and *Xmn*I, and loaded into lane 3 to lane 6. *Nco*I and *Xmn*I digested the pTS12 at 415 and 2319 base locations which produced two 803-bp and 1904-bp DNA fragments (lane 3). However, only *Xmn*I digested pUC19 at 2298 base and produced a linear DNA strand of 2686 bp (lane 4). Similarly, as *Sma*I and *Xmn*I were used, only *Xmn*I digested pTS12 at 2319 base and produced a linear DNA fragment of 2707 bp (lane 5), while both *Sma*I and *Xmn*I digested pUC19 at 414 and 2298 base locations and produced two DNA fragments of 802 bp and 1884 bp (lane 6).

Assessment of binding efficiency of bis-PNA

To explore the binding efficiency of bis-PNA-plasmid complex, different concentration of bis-PNA was hybridized with the plasmid and the electrophoresis mobility shift assay (EMSA) was performed [22]. Bis-PNA probe was serially diluted (50 μM, 30 μM, 20 μM, 10 μM, 5 μM, 1 μM) and hybridized with 200 pM of pTS12 in the hybridization buffer (10 mM Na_3PO_4, 1 mM EDTA in DI water, pH 7), at 42 °C overnight. Following the triplex formation, the construct was double digested with *EcoR*I and *Sap*I restriction enzymes to cut the hybridized segments. Gel-shift analyses were carried out in 8% polyacrylamide gel containing SYBR™ Safe DNA Gel staining, under 50 V for 3 h. UV transilluminator results in Fig. 2 showed that the samples hybridized with a higher concentration of bis-PNA probes had less mobility and the highest mobility was achieved in the case of sole plasmid represented as the control.

Mitochondrial DNA construction

MtDNA was isolated from skin-derived fibroblasts using the Puregene kit. The mutant mtDNA sample had the adenine (A) to guanine (G) transition at position 3243 (m3243A>G). To perform the SNP detection on a double-stranded DNA, initially, a PCR amplification procedure was performed to amplify a segment of wild-type and mutant mtDNA samples (108 bp) using two pairs of primer set (mt3212F: 5′CACCCAAG AACAGGGTTTGT3′ and mt3319R: 5′TGGGCCAT CCCTATGTTGTTAA3′). Further, to evaluate the detection limit of the system, the concentration of the mtDNAs was serially diluted in both target and control experiments. The experiments were repeated at the lowest concentration detection limit to evaluate the sensor's performance at a more realistic concentration if the PCR amplification was omitted.

Assay development and sensor assembly

Probe coupling and characterization of microspheres

One hundred microliters of carboxylic acid polystyrene beads (6.78×10^9/mL) was conjugated with 10 nmol of amine-functionalized bis-PNA probe and 10 nmol of amine-functionalized γ-PNA probe separately as previously reported [19]. To evaluate the conjugation chemistry procedure zeta potential of the negatively charged carboxylic acid polystyrene beads was measured prior and after the immobilization of the neutral PNA probes utilizing the NanoBrook Omni (Brookhaven Instruments Corp, Holtsville, NY). Zeta potential for carboxylic acid beads was − 60 ± 2.2 mV, followed by − 15 ± 4.0 mV for bis-PNA and − 25 ± 5.2 mV for γ-PNA-beads.

Hybridization assay

The probe-conjugated beads were washed three times with 0.4 × SSC buffer (60 mM NaCl, 6 mM trisodium citrate, 0.1%Triton X-100 in DI water, pH 8) and were re-suspended into 50 μL of hybridization buffer (10 mM Na_3PO_4, 1 mM EDTA in DI water, pH 7). In the case of pTS12, bis-PNA-beads were incubated with serially diluted pTS12 from 100 pM to 1 pM at 42 °C for 12 h and the control pUC19 was incubated with the bis-PNA-beads under the same concentrations and hybridization conditions. For the mtDNA experiments, serially diluted 100 pM to 1 pM wild type and mutant were incubated with the γ-PNA-beads in 50 μL of hybridization buffer (10 mM NaCl, 10 mM sodium phosphate, pH 7.5) at 68 °C for 12 h. After hybridization, the samples were washed three times with 0.4 × SSC buffer and suspended into 10 mM KCl, 10 mM HEPES, pH 7 solution for sensing measurements.

Sensor apparatus and electrical measurements

Micropipettes with 2-μm diameter were fabricated utilizing the laser-assisted puller-Sutter P 2000 with a pre-set program (Heat 350, Filament 4, Velocity 40, Delay 200, Pulling 0; Heat 350, Filament 4, Velocity 25, Delay 200, Pulling 0). The device assembly and the electrical measurements were attained as previously described [19]. Fifty microliters of electrolyte (10 mM KCl, 10 mM HEPES, pH 7) was backfilled into a micropipette and 30 V DC bias was applied across the pipette. The baseline current was stabilized and recorded for 1 min prior to the injection of probe-conjugated microspheres hybridized with target and control oligonucleotides into the pipettes. The conductance across the pipette was recorded using the LabVIEW program and the trajectory of the beads was monitored and recorded at the capturing frequency of 100

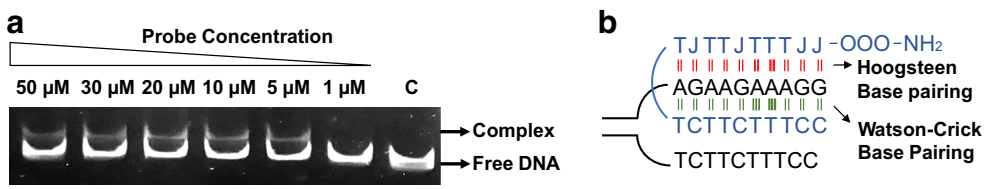

Fig. 2 **a** Electrophoresis mobility shift assay in 8% polyacrylamide gel. The following bis-PNA concentrations were used: 50 μM, 30 μM, 20 μM, 10 μM, 5 μM, 1 μM along with no bis-PNA as the control. **b** Schematic representation of plasmid and complementary bis-PNA invasion, forming a triplex complex

frames/s utilizing a high-resolution camera (Andro Neozyla 5.5) under an inverted microscope (Nikon Eclipse TE2000-E). Every experiment was repeated for at least 10 times by reversing the voltage polarity in a freshly pulled pipette.

Results and discussion

In the work presented here, we designed bis-PNA and γ-PNA probe assays for the detection of sequence-specific circular DNA and mtDNA with SNPs by utilizing an electrokinetic-based sensor developed by our team [19]. Neutral in charge, bis-PNA and γ-PNA specifically can bind with double-stranded nucleic acids to form the triplex construct (Fig. 3a) and have been extensively used for in vitro and in vivo identification of double-stranded DNAs [23–26]. Bis-PNA can bind with the complementary DNA to form stable (PNA)2/DNA triplex, with high thermal stability and resistance to harsh pH environment [27]. Also, γ-PNA possesses various advantages such as high affinity to complementary nucleic acid targets, enhanced water solubility, and capability to invade double-stranded DNA to form triplex helix [28].

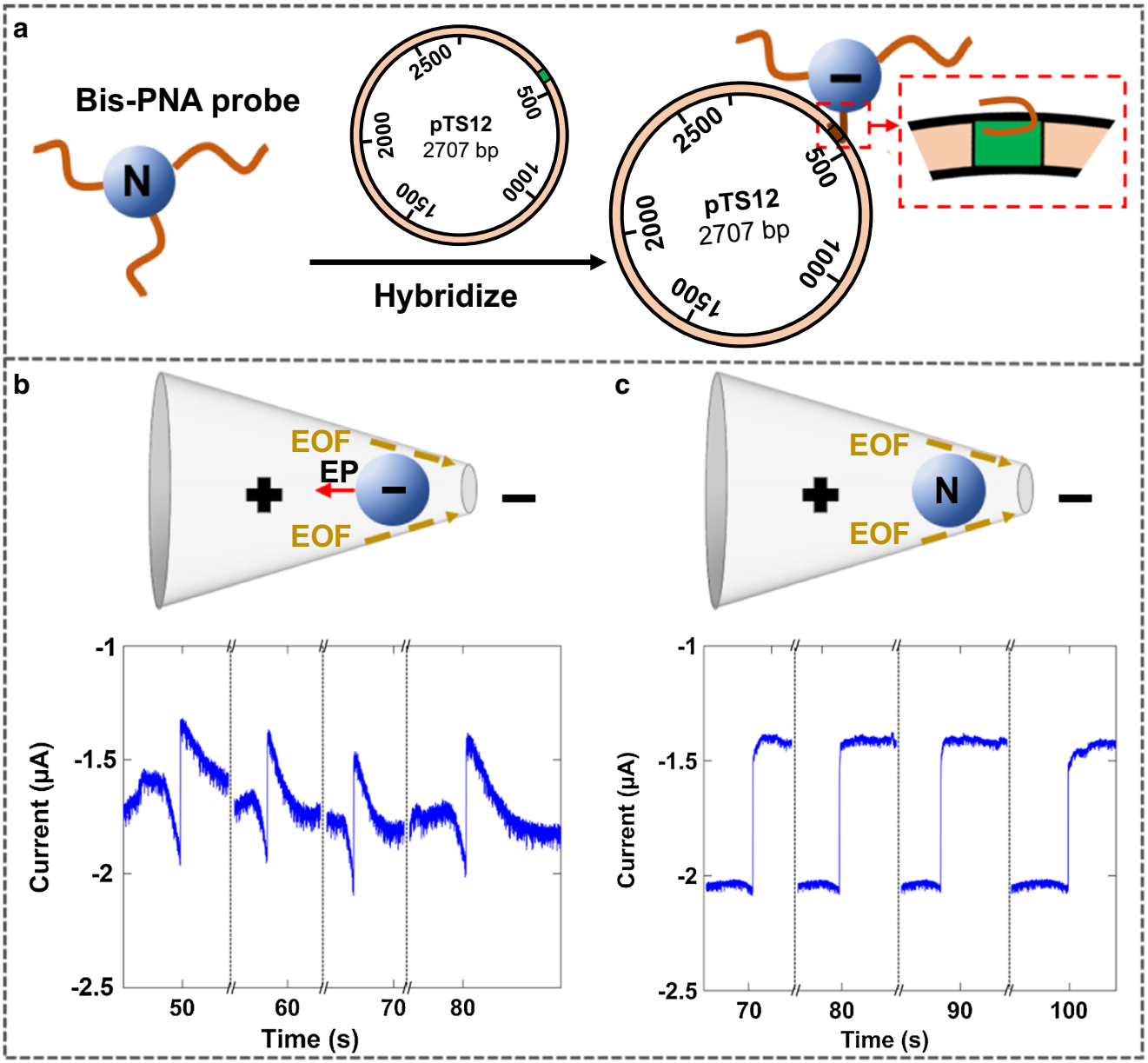

Fig. 3 **a** Schematic of triplex construct as the bis-PNA hybridized with double-stranded circular pTS12 plasmid and the transformation of a neutral bead to a negatively charged complex. **b** pTS12-PNA-bead complex was driven to the pore under the electroosmotic force (EOF) and the serrated shaped electrical signals were obtained. **c** Control bis-PNA-bead incubated with the non-complementary pUC19 plasmid was driven under EOF and the right-angled electrical signals were obtained

Circular plasmid detection

As a model system for the detection of an intact double-stranded circular mtDNA, recombinant plasmid pTS12 was constructed by insertion of the target gene into the pUC19 plasmid. Sensing experiments were conducted with pTS12 as the target and pUC19 as the control upon hybridization of the plasmids with bis-PNA-beads. The electroosmosis was induced as the driving force to translocate the target and control samples toward the pipette's tip (sensing zone) which resulted in pore blockades and distinguishable electrical conductance changes (Fig. 3b and c). The unique and distinguishable serrated-shape signals obtained by the target (Fig. 3b), demonstrates the capability of the system to detect the sequence-specific circular DNA via bis-PNA assay. The serrated-shape signal can be divided into three segments including the gradual current increase as the bead reached the sensing zone which caused by the particle-induced ionic concentration polarization effect [29]; the current drop, because of the pore blockade by the bead; and the current increase due to the strong opposite electrophoretic force at the tip induced on the negatively charged bead and, thus, the pore re-opening. However, right-angled current traces were attained in the control experiments with pUC19-PNA-beads (Fig. 3c) and sole PNA-beads (data not shown). The right-angled signals could be justified by either insufficient charge on the bead or the removal of the loosely bound non-specific DNAs under the strong electric field at the tip. Another control experiment was run utilizing the carboxylic acid beads in the absence of immobilized probes and hybridized oligonucleotides. As the highly negatively charged beads were driven toward the pore by the electroosmosis flow, the strong opposing electrophoretic force halted the forward motion of the beads toward the sensing zone, and thus no current blockades were obtained and confirmed microscopically, similar to our previously reported observation [19].

To further investigate the limit of detection (LOD) of our system, experiments were repeated as the plasmids were serially diluted from 100 pM, 10 pM, to 1 pM, and the number of serrated and right-angled blockades were counted for each concentration (Table 1). The results illustrate that as the concentration of the plasmid decreased to 1 pM, only the right-angled blockades were observed in the target experiments, which signifies the LOD of our system as 10 pM. The picomolar LOD obtained in these experiments compared to our previously reported femtomolar LOD with single-stranded nucleic acids [18, 19] could be due to the steric hindrance effect; the hybridization between the circular plasmid and the immobilized PNA was hindered by the large area of single plasmid, and thus the latter plasmid could hardly reach to the next PNA probe.

Table 1 LOD of the system for the detection of the pTS12 plasmid

Concentration (pM)	pTS12		pUC19	
	No. of serrated signal	No. of right-angled signal	No. of serrated signal	No. of right-angled signal
100	19	0	0	19
10	16	0	1	13
1	0	18	0	13

Detection of mtDNA point mutations

To investigate the specificity of our sensor for the detection of SNPs on a double-stranded DNA, mtDNAs with a single-base mismatch (m.3243A>G) located at the displacement-loop (D-loop) was utilized. The m.3243A>G is one of the most common mtDNA mutations, which could cause maternally inherited diabetes and deafness (MIDD) and mitochondrial encephalopathy with lactic acidosis and stroke-like episodes (MELAS) [30]. In these experiments, wild-type and mutant mtDNAs were serially diluted from 100 pM, 10 pM, to 1 pM and hybridized with γ-PNA probes immobilized on the beads. Similar to the above experiments, target and control beads were driven toward the pore under the EOF and the distinguishable electric signals were obtained. The LOD of the system for mtDNA was established as 10 pM, approximately ~ 10^8 mtDNA copies, which is translatable to around 10^4 to 10^6 cells. The relatively low number of cells that are required per measurement potentially enables the successful detection of mtDNAs from initial tissue biopsy without the need for laborious and time-consuming cell culture procedure. To further set the accuracy of our system at the low concentration detection, the number of serrated and right-angled blockades in the target and control experiments were counted. In the case of the target, 15 serrated blockades out of 17 blocks were obtained, and in the case of the control, 10 right-angled blockades out of 12 blocks were counted which represents an estimation of 86.2% accuracy of our platform. Although the accuracy of our system is lower than the conventional mtDNA detection techniques, we believe that in future, it can be improved by optimizing the hybridization conditions including the stringency, the chamber volume, and addition of a micro-mixer.

Conclusion

This work represents a new class of bioanalytical tools for the detection of sequence-specific circular double-stranded DNA with single-base mismatch specificity at the picomolar concentration detection limit. The novel bis-PNA and γ-PNA assays utilized in this technique have significantly simplified the sample preparation procedure and, thus, greatly reduced the cost and time of the detection. In future, this PCR-independent, deployable, and semi-automated sensor can be

integrated with microfluidics to be evolved as a complete point-of-care (POC) system for rapid, sensitive, and cost-effective screening of mitochondrial DNA genome in the clinical and forensic research.

Acknowledgements The authors thank Shiyu Luo from Dr. Huang's group for the generous help on mitochondrial DNA preparation.

Compliance with ethical standards

Conflict of interest The authors declare that they have no conflict of interest.

References

1. Andersson GE, Karlberg O, Canbäck B, Kurland CG. On the origin of mitochondria: a genomics perspective. Philos Trans Royal Soc B Biol Sci. 2003;358(1429):165–79.
2. Taylor RW, Turnbull DM. Mitochondrial DNA mutations in human disease. Nat Rev Genet. 2005;6:389.
3. Parr RL, Martin LH. Mitochondrial and nuclear genomics and the emergence of personalized medicine. Hum Genomics. 2012;6(1):3.
4. Melton T, Nelson K. Forensic mitochondrial DNA analysis: two years of commercial casework experience in the United States. Croat Med J. 2001;42(3):298–303.
5. Palo JU, Hedman M, Söderholm N, Sajantila A. Repatriation and identification of Finnish World War II soldiers. Croat Med J. 2007;48(4):528.
6. Meierhofer D, Mayr JA, Ebner S, Sperl W, Kofler B. Rapid screening of the entire mitochondrial DNA for low-level heteroplasmic mutations. Mitochondrion. 2005;5(4):282–96.
7. Wong L-JC, Chen T-J, Tan D-J. Detection of mitochondrial DNA mutations using temporal temperature gradient gel electrophoresis. Electrophoresis. 2004;25(15):2602–10.
8. Cassandrini D, Calevo MG, Tessa A, Manfredi G, Fattori F, Meschini MC, et al. A new method for analysis of mitochondrial DNA point mutations and assess levels of heteroplasmy. Biochem Bioph Res Co. 2006;342(2):387–93.
9. Li M, Schönberg A, Schaefer M, Schroeder R, Nasidze I, Stoneking M. Detecting heteroplasmy from high-throughput sequencing of complete human mitochondrial DNA genomes. Am J Hum Genet. 2010;87(2):237–49.
10. Maitra A, Cohen Y, Gillespie SE, Mambo E, Fukushima N, Hoque MO, et al. The human MitoChip: a high-throughput sequencing microarray for mitochondrial mutation detection. Genome Res. 2004;14(5):812–9.
11. Taylor P, Manage DP, Helmle KE, Zheng Y, Glerum DM, Backhouse CJ. Analysis of mitochondrial DNA in microfluidic systems. J Chromatogr B. 2005;822(1):78–84.
12. Shi M, Zheng J, Tan Y, Tan G, Li J, Li Y, et al. Ultrasensitive detection of single nucleotide polymorphism in human mitochondrial DNA utilizing ion-mediated cascade surface-enhanced Raman spectroscopy amplification. Anal Chem. 2015;87(5):2734–40.
13. Sun L, Hu N, Peng J, Chen L, Weng J. Ultrasensitive detection of mitochondrial DNA mutation by graphene oxide/DNA hydrogel electrode. Adv Funct Mater. 2014;24(44):6905–13.
14. Song Y, Gyarmati P, Araújo AC, Lundeberg J, Brumer H, Ståhl PL. Visual detection of DNA on paper chips. Anal Chem. 2014;86(3):1575–82.
15. Chang C-M, Chiu L-F, Wang P-W, Shieh D-B, Lee G-B. A microfluidic system for fast detection of mitochondrial DNA deletion. Lab Chip. 2011;11(16):2693–700.
16. Chang C-M, Chiu L-F, Wei Y-H, Shieh D-B, Lee G-B. Integrated three-dimensional system-on-chip for direct quantitative detection of mitochondrial DNA mutation in affected cells. Biosens Bioelectron. 2013;48:6–11.
17. Esfandiari L, Monbouquette HG, Schmidt JJ. Sequence-specific nucleic acid detection from binary pore conductance measurement. J Am Chem Soc. 2012;134(38):15880–6.
18. Esfandiari L, Lorenzini M, Kocharyan G, Monbouquette HG, Schmidt JJ. Sequence-specific DNA detection at 10 fM by electromechanical signal transduction. Anal Chem. 2014;86(19):9638–43.
19. Zhang Y, Rana A, Stratton Y, Czyzyk-Krzeska MF, Esfandiari L. Sequence-specific detection of MicroRNAs related to clear cell renal cell carcinoma at fM concentration by an electroosmotically driven nanopore-based device. Anal Chem. 2017;89(17):9201–8.
20. Esfandiari L, Wang S, Wang S, Banda A, Lorenzini M, Kocharyan G, et al. PCR-independent detection of bacterial species-specific 16S rRNA at 10 fM by a pore-blockage sensor. Biosensors. 2016;6(3):37.
21. Green MR, Sambrook J, Sambrook J. Molecular cloning: a laboratory manual, 4th ed. New York: Cold Spring Harbor Laboratory Press; 2012. p.1233–37.
22. Smith MF, Delbary-Gossart S. Electrophoretic mobility shift assay (EMSA). In: M S, editor. Colorectal Cancer: methods and protocols. Totowa: Humana Press; 2001. p. 249–57.
23. Nielsen PE. Targeting double-stranded DNA with peptide nucleic acid (PNA). Curr Med Chem. 2000;8(5):545–50.
24. Kuhn H, Sahu B, Rapireddy S, Ly DH, Frank-Kamenetskii MD. Sequence specificity at targeting double-stranded DNA with a γ-PNA oligomer modified with guanidinium G-clamp nucleobases. Aritf DNA PNA XNA. 2010;1(1):45–53.
25. Zelphati O, Liang X, Hobart P, Felgner PL. Gene chemistry: functionally and conformationally intact fluorescent plasmid DNA. Hum Gene Ther. 1999;10(1):15–24.
26. Chen J, Peterson KR, Iancu-Rubin C, Bieker JJ. Design of embedded chimeric peptide nucleic acids that efficiently enter and accurately reactivate gene expression in vivo. Proc Natl Acad Sci. 2010;107(39):16846–51.
27. Coull J, Deuholm KL, Christensen L, Egholm M, Buchardt O, Nielsen PE. Efficient pH-independent sequence-specific DNA binding by pseudoisocytosine-containing bis-PNA. Nucleic Acids Res. 1995;23(2):217–22.
28. Sahu B, Sacui I, Rapireddy S, Zanotti KJ, Bahal R, Armitage BA, et al. Synthesis and characterization of conformationally preorganized, (R)-diethylene glycol-containing γ-peptide nucleic acids with superior hybridization properties and water solubility. J Org Chem. 2011;76(14):5614–27.
29. Qiu Y, Lin C-Y, Hinkle P, Plett TS, Yang C, Chacko JV, et al. Highly charged particles cause a larger current blockage in micropores compared to neutral particles. ACS Nano. 2016;10(9):8413–22.
30. Greaves LC, Reeve AK, Taylor RW, Turnbull DM. Mitochondrial DNA and disease. J Pathol. 2012;226(2):274–86.